Optimal Coherent Filtering for Single Noisy Photons

S. Gao,[1] O. Lazo-Arjona,[1] B. Brecht,[1,2] K. T. Kaczmarek,[1,3] S. E. Thomas,[1,4] J. Nunn,[5] P. M. Ledingham,[1] D. J. Saunders,[1,*] and I. A. Walmsley[1,†]

[1]*Clarendon Laboratory, University of Oxford, Parks Road, Oxford OX1 3PU, United Kingdom*
[2]*Integrated Quantum Optics, Universität Paderborn, Warburger Strasse 100, 33098 Paderborn, Germany*
[3]*Groupe de Physique Appliquée, Université de Genève, CH-1211, Genève, Switzerland*
[4]*QOLS, Blackett Laboratory, Imperial College London, London SW7 2BW, United Kingdom*
[5]*Centre for Photonics and Photonic Materials, Department of Physics, University of Bath, Claverton Down, Bath BA2 7AY, United Kingdom*

(Received 20 February 2019; published 20 November 2019)

We introduce a filter using a noise-free quantum buffer with large optical bandwidth that can both filter temporal-spectral modes as well as interconvert them and change their frequency. We theoretically show that such quantum buffers optimally filter out temporal-spectral noise, producing identical single photons from many distinguishable noisy single-photon sources with the minimum required reduction in brightness. We then experimentally demonstrate a noise-free quantum buffer in a warm atomic system that is well matched to quantum dots. Based on these experiments, simulations show that our buffer can outperform all intensity (incoherent) filtering schemes for increasing indistinguishability.

DOI: 10.1103/PhysRevLett.123.213604

Single photons are required for many quantum technologies [1], for example, quantum communication [2], quantum metrology [3], optical quantum computing [4], and quantum networks [5]. There are three key metrics to characterize single-photon sources: (1) single-photon purity, characterized by the second-order intensity autocorrelation function $g^{(2)}(\tau = 0)$, where τ is the time delay between two arms of a Hanbury Brown–Twiss interferometer; (2) brightness (B), which is the probability of having one photon per trial, defined at or after collection optics; (3) indistinguishability. In this Letter, we define two kinds of indistinguishability: (a) self-indistinguishability $I^{(1)}$, describing the Hong-Ou-Mandel (HOM) dip visibility of photons coming from the same photon source generated at different times, and (b) interindistinguishability $I^{(2)}$, referring to the HOM dip visibility of photons from different sources. $I^{(1)}$ and $I^{(2)}$ are determined by the purity and similarity of the quantum state of the photon in its complete specification [6] (i.e., both modal and in the basis state expansion, e.g., Fock states). A perfect single-photon source is characterized by $g^{(2)}(0) = 0$, $B = 1$, $I^{(1)} = 1$, and $I^{(2)} = 1$.

Recently, steady progress has been made for single-photon sources with near ideal single-photon statistics and high brightness [7,8]. Regarding indistinguishability, the critical remaining factor that limits this is the mixing of temporal optical modes due to numerous additional undesired physical processes (see review: Ref. [9]) in most single-photon emitters such as defects in the solid state [10]. To circumvent this issue, it is common to filter the photons after emission. However, passive intensity filtering only achieves at best $I^{(1)}$, $I^{(2)} \to 1$ in the limit of $B \to 0$ [11]. To understand this and to illustrate how we overcome this problem, consider the normalized density matrix ρ which represents the temporal-spectral degrees of freedom of the photon, $\rho = \sum \alpha_k |\psi_k\rangle\langle\psi_k|$, where $|\psi_k\rangle$ are single-photon excitations of the respective temporal eigenmodes $\psi_k(t)$. The indistinguishability of the photon is unity when ρ has only one nonzero eigenvalue, i.e., it is in a single temporal-spectral mode [12]. A mixed state has $I^{(1)} < 1$ and comprises multiple field-orthogonal, but intensity-nonorthogonal, eigenmodes. Therefore, an intensity (temporal or spectral) filter can only selectively pass a single mode within a mixed state in the limit of infinitesimally narrow passband, which necessarily reduces the brightness of the selected mode to zero. In this Letter, we propose a coherent filter—a quantum buffer—which can remove higher-order temporal modes of a single photon without detriment to the main eigenmode, increasing indistinguishability to unity while minimizing the reduction in brightness.

The basic operating principle of a quantum buffer is shown in Fig. 1. A buffer is placed after each single-photon source to delay a user-specified temporal-spectral wave packet, or temporal mode. In practice this should be the dominant ($k = 0$) eigenmode $|\psi_0\rangle$ with the largest eigenvalue α_0. All other modes ($k \geq 1$) are transmitted and time separated from the buffered mode ($k = 0$) with a buffer time T_{buff}, so it can be removed. As a result, the output of our quantum buffer will be in a pure state. If all the other degrees of freedom of the emission are identical and the second-order correlation function $g^{(2)}(0)$ of the buffered photons remains at zero, $I^{(1)} = 1$ would be achieved. An ideal quantum buffer selects the dominant eigenmode

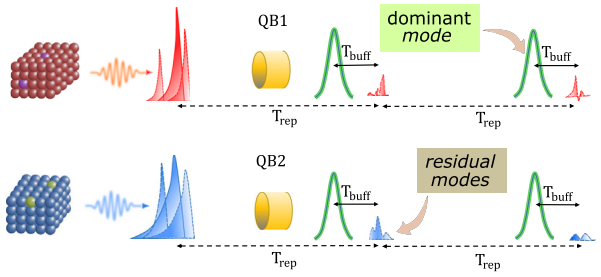

FIG. 1. Two single-photon sources emit photons that are in mixed states ($I^{(1)} < 1$) and in different sets of temporal-spectral modes ($I^{(2)} < 1$). After filtering with the quantum buffers (QB), the dominant mode and the residual modes are separated by a short programmable delay T_{buff}, and pure ($I^{(1)} = 1$) and identical photons ($I^{(2)} = 1$) are recalled by filtering out the residual noisy modes.

with unit efficiency, and therefore the brightness will decrease proportional to the largest eigenvalue, $B_{\text{out}} = \alpha_0 B_0$, where B_0 is the brightness of the single-photon source before the quantum buffer. Since different sources may have different dominant temporal modes $|\psi_0\rangle$, the filtered mode will differ from source to source. An ideal quantum buffer will unify these modes, producing the same output mode $|\phi\rangle$ for every single-photon source, making both $I^{(1)}$ and $I^{(2)}$ unity.

Devices that can select particular temporal modes have been demonstrated previously [13–17]; however, careful engineering of the underlying nonlinear operation is required to suppress spurious noise processes and render noise levels quantum compatible. Furthermore, phase-matching constraints make the operational bandwidth too large for the gigahertz bandwidths of leading photon sources [8,18]. Here we describe a noise-free gigahertz-band quantum buffer based on the off-resonant-cascaded-absorption (ORCA) buffer protocol in atomic alkali vapors, closely related to our recent demonstration of a noise-free ORCA quantum memory in warm caesium (Cs) vapor [19]. The ORCA protocol is based on reversible coherent off-resonant two-photon absorption in an atomic ensemble. An input signal, such as a quantum dot (QD)-emitted photon with temporal-spectral mode $S(z,t)$, is stored into a delocalized atomic coherence $B(z,t)$ shared between the ground and doubly excited state across the ensemble, mediated by a strong control field $\Omega_{\text{in}}(z,t)$ [see Fig. 2(b)]. This atomic coherence is then reversibly read out of the buffer on demand back into an optical signal by application of a second control field $\Omega_{\text{out}}(z,t)$ after a short buffering time.

The interaction is described by the equations (see Supplemental Material II [20])

$$\partial_t B(z,t) = -\frac{|\Omega(z,t)|^2}{\Gamma_2} B(z,t) - i\kappa \frac{\Omega(z,t)^*}{\Gamma_1} S(z,t),$$
$$\left(\partial_z + \frac{1}{c}\partial_t\right) S(z,t) = -\frac{i\kappa^* \Omega(z,t)}{\Gamma_2} B(z,t), \quad (1)$$

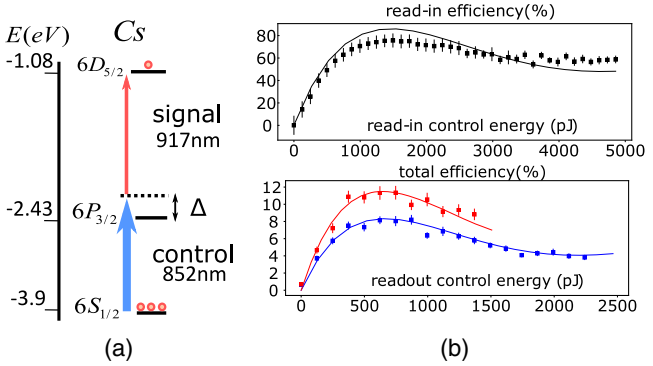

FIG. 2. (a) Atomic transitions of the ORCA buffer. Δ is the frequency detuning from single-photon resonance. (b) Buffer efficiency for different read-in and readout control pulse power, calculated by comparing the ratio photon counts with and without the control pulse active for the read-in and readout time bins. Solid line is given by the theory in Supplemental Material II [20]. Squares with error bars are experimental data. We show total efficiency for different read-in control powers in the lower figure: blue for ~700 pJ and red for ~1310 pJ.

where Γ_1 and Γ_2 are the spontaneous decay rates of the intermediate state and doubly excited state. κ is the light-matter coupling constant including the transition dipole moment and atomic number density. This is a linear interaction; therefore the mapping of light $S_{\text{in}}(t)$ to atoms $B(z)$ and then atoms $B(z)$ back to light $S_{\text{out}}(t)$ can be described via the Green's functions:

$$B(z) = \int G_{\text{in}}(z,t) S_{\text{in}}(t) dt,$$
$$S_{\text{out}}(t) = \int G_{\text{out}}(t,z) B(z) dz. \quad (2)$$

The Green's functions can either be numerically calculated (see Supplemental Material II [20]) or tomographically measured [25]. A singular value decomposition of the input Green's function, $G_{\text{in}}(z,t) = \sum_k \lambda_k^{\text{in}} b_k(z) u_k^*(t)$, will give a series of orthogonal input signal modes $u_k(t)$ mapping to orthogonal atomic coherence modes $b_k(z)$ with a read-in efficiency equal to the square of the corresponding singular value λ_k^{in}. A *single-mode* interaction has a Green's function with only one nonzero singular value λ_0^{in}, meaning that there is only one input mode $u_0(t)$ that interacts with the ORCA buffer. Since the Green's function G_{in} is determined by the temporal-spectral mode of the control field $\Omega^{\text{in}}(t)$ [26,27], we can engineer the ORCA buffer by pulse shaping the control field such that $u_0(t)$ matches the dominant mode $\psi_0(t)$ of a QD single-photon source emission. In practice, the required control field pulse shape is found numerically by an optimization algorithm. In the same way, we can manipulate G_{out} such that the output mode of the ORCA buffer is a user-defined one to match emissions from different single-photon sources.

The ORCA protocol can be a single-mode operation for optimized parameters, such as atomic medium length,

detuning, control field energy, and temporal shape [28], or if operated in a low-finesse cavity [29]. In the general case, the output of an ORCA buffer can be a mixture of different modes described by the density matrix,

$$\rho_{\text{out}} = \frac{1}{W}\sum_k \xi_k \alpha_k |v_k\rangle\langle v_k|, \tag{3}$$

where ξ_k is the buffer efficiency for the quantum state $|\psi_k\rangle \to |v_k\rangle$ with $W = \sum_k \xi_k \alpha_k$ (normalization constant). The brightness after the buffer is $B = W$; the indistinguishability of the output photon will be $I_{\text{out}} = 1/K_{\text{out}} = \text{Tr}[\rho_{\text{out}}^2]$, where K is the Schmidt number [30].

For an experimental realization we consider ORCA with Cs [see Fig. 2(a)]. Here, we apply the control field off-resonantly to the $D2$ line ($S_{1/2} \to P_{3/2}$) resonance, counter-propagating with the signal which is applied to $P_{3/2} \to D_{5/2}$ [Fig. 2(b)]. This signal transition (917 nm) is of particular interest as it is well matched to many state-of-the-art quantum dots single-photon sources; see, e.g., Ref. [7]. To pinpoint the exact frequency, we can adjust the detuning of the control field, such that the two-photon resonance condition matches the source emission. Furthermore, like the ORCA memory, the bandwidth of the ORCA buffer is set by that of the control field, and can easily accommodate the gigahertz band of many single-photon sources [7]. However, in contrast to the ORCA memory, the buffer uses a control field tuned closer to the populated atomic resonance, thus potentially inducing spontaneous Raman scattering into the signal mode. This process could potentially contaminate the single-photon purity. Therefore, as a first step toward temporal-spectral filtering, we verify the noise-free operation of the ORCA buffer with a proof-of-principle experiment (see Supplemental Material I [20] for details).

Using a strong classical laser pulse as a control, we store and recall weak coherent states from our quantum buffer: an ensemble of Cs atoms in a vapor cell held at ~100 °C. The strong control field is detuned from the intermediate atomic state by $\Delta = 7.5$ GHz; see Fig. 2(a), and for details see Supplemental Material I [20]. At a buffer time of 5.5 ns we observe total efficiencies $\eta_{\text{out}} > 10\%$ and noise-free performance with $\mu_1 < (1 \pm 0.06) \times 10^{-4}$ (where $\mu_1 =$ noise over efficiency, a common measure of memory performance [31]). The effect on photon number purity caused by any residual noise in our buffer can be shown to be $g^{(2)}(0)_{\text{output}} \approx 2\mu_1$ (see Supplemental Material I [20]), which is negligible given our measured μ_1. Furthermore, this small amount of noise is comparable with observed detector dark count rates, confirming that our Cs ORCA buffer itself is noise-free, as observed in our ORCA memory [19].

The excellent agreement seen between the data and Eqs. (1) in Fig 2(b) verifies our model (see Supplemental Material III [20] for data-fitting details). For the case of short buffer times, i.e., operating faster than the Doppler dephasing, we predict an efficiency for our current experiment of 34%, which is limited by the available control pulse energy, pulse shapes, and forward retrieval. However, the equations that govern our quantum buffer map onto those for Raman memories, which can reach 100% efficiency [26], therefore by increasing control power, changing the direction of the readout pulse, and optimizing pulse shapes can enable perfect buffering.

With the current ORCA buffer characterized, we move to numerically predict the coherent filtering performance of our current Cs ORCA buffer implementation for filtering solid-state single-photon source emission. The indistinguishability and the brightness are both determined by the *singlemodeness* of our ORCA buffer.

We consider the application of the buffer to gigahertz bandwidth quantum dot emission [7,32]. Semiconductor quantum dots are a leading single-photon source candidate, with unprecedented brightness and very low $g^{(2)}(0)$ [8,33–36]. However, QDs (as well as other solid-state sources [10]) suffer from fast local environmental fluctuations that contribute to pure dephasing of the QD. Furthermore, electron-phonon interactions will also result in the decoherence of each emitted photon, which limits the indistinguishability: $I^{(1)} < 1$ even at 0 K and in the weak excitation regime [37,38]. To suppress these dynamics as well as to direct emission, QDs are typically embedded in waveguides [39,40] or microcavities [18,41–43]. However, there remains a trade-off between brightness and indistinguishability, as explored in Ref. [24].

We start by considering a single photon emitted by a QD. Its temporal-spectral mode is described by an intrinsic spectral field correlation function, $C(\omega,\mu)_{\omega_0,t_0} = \langle E^+(\omega)E(\mu)\rangle_{\omega_0,t_0}$, where E^+ and E are the creation and annihilation operators of the electric field, and ω_0 and t_0 are the central frequency and emission time. This function describes to lowest order the output of a QD source that suffers from pure dephasing and electron-phonon interactions which sets the ultimate fundamental limit of indistinguishability of QD emission [24]. The single-photon density matrix is the normalized intrinsic two-color correlation function in matrix form: $\rho_{\text{itr}}^{\omega\mu} = C(\omega,\mu)/M$, with $M = \int C(\omega,\omega)d\omega$ [20]. The QD emission may also suffer from spectral diffusion [44–47] and temporal jitter, which are induced by both the host material and excitation scheme. The general form of the total density matrix of the emitted photons will be

$$\rho = \int p(t_0,\omega_0)\rho_{\text{itr}}(\omega_0,t_0)dt_0 d\omega_0, \tag{4}$$

where $p(t_0,\omega_0)$ is a probability distribution capturing any inhomogeneous broadening. The Fourier transform of the spectral correlation function is the two-time correlation function which, in practice, can be measured without any detailed knowledge about the noise dynamics of the source. (see Supplemental Material IV [20]).

We analyze the effectiveness of the ORCA buffer as a single-mode selective operation by simulating a state-of-the-art off-resonantly excited QD with a self-indistinguishability of $I^{(1)} \approx 0.7$ (similar to QD3 in Ref. [18]) and predicting the improvement in single-photon indistinguishability with our Cs ORCA buffer using the same parameters as our experiments. Here the distinguishability of the QD is mainly caused by timing jitter induced by the off-resonant pumping scheme. Figure 4(a) shows the modal distribution of this QD as well as the modal distribution post filtering. Note that the $k = 0$ mode is delivered with high efficiency while the $k \geq 1$ modes are highly suppressed, indicating that the ORCA buffer is very near a single-mode operation. We predict an increase of the indistinguishability to $I^{(1)}_{\text{out}} \approx 0.98$, with a brightness of $B_{\text{out}} = 0.4B_0 \approx 0.29$, where $B_0 = 0.72$ is the initial brightness of the QD [orange bars in Fig. 4(a)]. This predicted performance already matches the leading resonantly pumped QDs (e.g., QD4 in Ref. [18]). To improve performance even further, we numerically optimize the shape and energy of both the read-in and readout control pulse. The brightness and self-indistinguishability after buffering then is $I^{(1)}_{\text{out}} \approx 0.98$, $B_{\text{out}} \approx 0.61B_0 \approx 0.43$ [blue bars in Fig. 4(a)].

An important property of the buffer is its ability to outperform passive filtering (i.e., a time-stationary linear filter) when delivering pure single-photon states. We therefore compare our predicted ORCA temporal-spectral filtering against this conventional passive intensity filtering approach [48,49] for QD emission at the input. To explore this landscape, we simulate 16 different QDs with various pure dephasing magnitudes, spectral diffusion, and timing jitter (see Supplemental Material V [20] for parameter details). The performance of passive intensity filtering is shown in Fig. 3, where unit indistinguishability can only be achieved in the limit that the brightness goes to zero. The upper bound of the intensity filter region is found by simulating 100 QDs with various noise dynamics (see Supplemental Material VI [20] for details about the intensity filter model). We also plot the predicted performance of our experimental demonstration of the ORCA buffer system, both with and without control-pulse shape optimization; both outperform passive filtering. An ideal filter would have $I^{(1)} = 1$ and $B = B_0\alpha_0$. We have shown that the equations of motion for the ORCA buffer allow for unit memory efficiencies, with $K = 1$ [28], which with proper mode matching can optimally filter QD emission. To improve the predicted performance closer to an ideal quantum buffer, additional numerical optimization is required, for example, adjusting the interaction length and temperature, or implementing our ORCA buffer in a low-finesse cavity [29].

Besides improving the self-indistinguishability $I^{(1)}$, our quantum buffer can convert the input temporal-spectral mode to an arbitrary output mode via reshaping of the readout control field, thereby mode matching emission

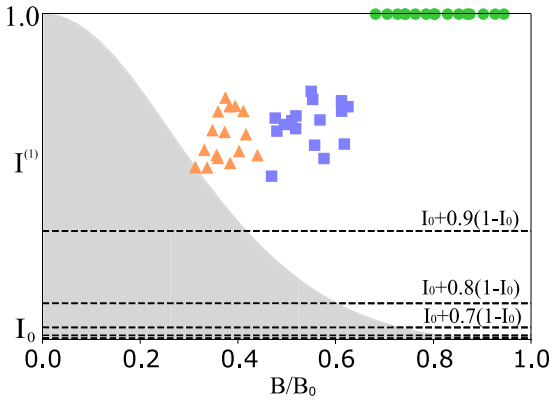

FIG. 3. Filtering simulation. The shaded area indicates the simulated intensity filtering. We plot the brightness B normalized by the initial brightness B_0 against the self-indistinguishability $I^{(1)}$. I_0 is the initial self-indistinguishability. The dashed lines indicate $I^{(1)} = I_0 + q(1 - I_0)$, with q being a fraction indicating the improvement of $I^{(1)}$. The triangles indicate ORCA buffer filtering with Gaussian temporal-mode control pulse for 16 random samples. The squares are ORCA buffer filtering with optimized control pulse shape and energy for the same set. The circles show the performance of an ideal quantum buffer.

from disparate QDs. We demonstrate this capability numerically by modeling two distinct QD emissions with the same central frequency with an interindistinguishability of $I^{(2)} = 0.62$, as in Fig 4(b). We then simulate two ORCA buffers, one interacting with each QD. By selecting the largest eigenmode of each QD in their respective ORCA buffers using necessarily different read-in fields, and then recalling them with the same appropriately adjusted readout

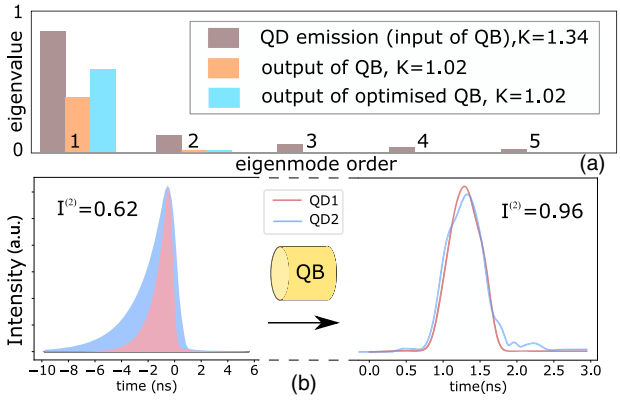

FIG. 4. (a) Simulation of singlemodeness of an ORCA buffer based on the demonstrated experimental performance in Fig. 2. We show the first 5 eigenvalues or modes before (brown) and after (orange and blue) the ORCA buffer. K is the Schmidt number (mode number). (b) Mode unification by an ORCA buffer. Emission from two distinct QDs ($I^{(2)} = 0.62$) with different decay times (left-hand figure) are actively unified by an ORCA buffer into two nearly identical photons (right-hand figure, $I^{(2)} = 0.96$).

control field shapes, the interindistinguishability would be $I^{(2)} = 0.96$, since the stored excitations are read out into nearly identical modes. In the typical case where the different QD outputs are also distinguishable in their central emission frequency, it is possible using the ORCA protocol to adjust the readout frequency of the stored excitation as compared to the input. Our simulations show that frequency conversion up to 1 nm can be implemented without significant drop in efficiency (see Supplemental Material VII [20]). By combining coherent temporal-mode filtering and frequency conversion in a single device, this approach would overcome a key barrier to scaling photonic quantum technologies demanding many identical pure state single photons.

In conclusion, we have introduced a quantum buffer that can optimally filter the output from solid-state single-photon emitters. This provides a means to circumvent the distinguishability between photons generated sequentially from a single source or in parallel from different sources, due to temporal-spectral mode mixing ($I^{(1)} < 1$) and source-dependent mode mismatch ($I^{(2)} < 1$). We experimentally demonstrated the noise performance criteria for a quantum buffer in Cs vapor. Our noise-free Cs ORCA buffer is compatible in wavelengths and bandwidths with state-of-the-art InGaAs QDs, and will enable different QD emission from remote samples to be quantum buffered into pure and identical single-photon sources with no increase in $g^{(2)}(0)$. The ideas presented here are applicable to any noisy optical state and any photon source. Importantly, the room-temperature quantum buffer circumvents the limitations of passive frequency filtering and provides a new route to produce identical single photons from imperfect single-photon sources.

We would like to acknowledge Jake Iles Smith for providing a solver for QDs in cavity with pure dephasing and electron-phonon interaction, Pascale Sennellart for discussion on quantum dot operation and performance, Christian Weinzetl for comments on the manuscript, and Bryn Bell for useful discussion. We also thank Jonas Becker for discussions on noise mechanisms and models for the quantum dots outputs. I. A. W. acknowledge support from the European Research Council, the UK Engineering and Physical Sciences Research Council (Project No. EP/K034480/1 and the Networked Quantum Information Technology Hub EP/M013243/1), an ERC Advanced Grant (MOQUACINO, Grant ID: 339918), and ERC Proof of Concept (BRiiGHT, Grant ID: 813242), and the Air Force Office of Scientific Research (Grant/Cooperative Agreement No. FA9550-17-1-0064). P. M. L. acknowledges financial support from a European Union Horizon 2020 Research and Innovation Framework Programme Marie Curie individual fellowship, Grant Agreement No. 705278. S. E. T is supported by EPSRC via the Controlled Quantum Dynamics CDT under Grants No. EP/G037043/1 and No. EP/L016524/1, S. G is supported by National University of Defence Technology of China and O. L.-A. is supported by Consejo Nacional de Ciencia y Tecnología, and Banco de México.

*dylan.saunders@physics.ox.ac.uk
†ian.walmsley@physics.ox.ac.uk

[1] I. A. Walmsley, Science **348**, 525 (2015).
[2] M. Krenn, M. Malik, T. Scheidl, R. Ursin, and A. Zeilinger, Quantum communication with photons, in *Optics in Our Time*, edited by M. D. Al-Amri, M. El-Gomati, Mohamed, and M. S. Zubairy (Springer International Publishing, Cham, 2016), pp. 455–482.
[3] E. O. Göbel and U. Siegner, Quantum Metrology: Foundation of Units and Measurements (Wiley-VCH Verlag GmbH & Co. KGaA, New York, 2015).
[4] J. L. O'Brien, Science **318**, 1567 (2007).
[5] H. J. Kimble, Nature (London) **453**, 1023 (2008).
[6] J. P. Torres, K. Banaszek, and I. A. Walmsley, Prog. Opt. **56**, 227 (2011).
[7] P. Senellart, G. Solomon, and A. White, Nat. Nanotechnol. **12**, 1026 (2017).
[8] L. Schweickert, K. D. Jöns, K. D. Zeuner, S. F. C. da Silva, H. Huang, T. Lettner, M. Reindl, J. Zichi, R. Trotta, A. Rastelli, and V. Zwiller, Appl. Phys. Lett. **112**, 093106 (2018).
[9] M. D. Eisaman, J. Fan, A. Migdall, and S. V. Polyakov, Rev. Sci. Instrum. **82**, 071101 (2011).
[10] I. Aharonovich, D. Englund, and M. Toth, Nat. Photonics **10**, 631 (2016).
[11] P. J. Mosley, J. S. Lundeen, B. J. Smith, P. Wasylczyk, A. B. U'Ren, C. Silberhorn, and I. A. Walmsley, Phys. Rev. Lett. **100**, 133601 (2008).
[12] B. Brecht, D. V. Reddy, C. Silberhorn, and M. G. Raymer, Phys. Rev. X **5**, 041017 (2015).
[13] A. Eckstein, B. Brecht, and C. Silberhorn, Opt. Express **19**, 13770 (2011).
[14] V. Ansari, J. M. Donohue, B. Brecht, and C. Silberhorn, Optica **5**, 534 (2018).
[15] D. V. Reddy and M. G. Raymer, Optica **5**, 423 (2018).
[16] Y.-S. Ra, C. Jacquard, A. Dufour, C. Fabre, and N. Treps, Phys. Rev. X **7**, 031012 (2017).
[17] A. Shahverdi, Y. M. Sua, L. Tumeh, and Y.-P. Huang, Sci. Rep. **7**, 6495 (2017).
[18] N. Somaschi, V. Giesz, L. De Santis, J. C. Loredo, M. P. Almeida, G. Hornecker, S. L. Portalupi, T. Grange, C. Antón, J. Demory, C. Gómez, I. Sagnes, N. D. Lanzillotti-Kimura, A. Lemaítre, A. Auffeves, A. G. White, L. Lanco, and P. Senellart, Nat. Photonics **10**, 340 (2016).
[19] K. T. Kaczmarek, P. M. Ledingham, B. Brecht, S. E. Thomas, G. S. Thekkadath, O. Lazo-Arjona, J. H. D. Munns, E. Poem, A. Feizpour, D. J. Saunders, J. Nunn, and I. A. Walmsley, Phys. Rev. A **97**, 042316 (2018).
[20] See Supplemental Material at http://link.aps.org/supplemental/10.1103/PhysRevLett.123.213604 for a theoretical model of the ORCA buffer, experiment setup, data collection, noise analysis, Green's function analysis, modeling of quantum dot and intensity filtering, frequency conversion of

the ORCA buffer, and parameters used in both experiment as well as simulation, which includes Refs. [21–24].

[21] E. A. Goldschmidt, F. Piacentini, I. R. Berchera, S. V. Polyakov, S. Peters, S. Kück, G. Brida, I. P. Degiovanni, A. Migdall, and M. Genovese, Phys. Rev. A **88**, 013822 (2013).

[22] K. Kaczmarek, ORCA—Towards an integrated noise-free quantum memory, Ph.D. thesis, University of Oxford, 2017.

[23] K. T. Kaczmarek, P. M. Ledingham, B. Brecht, A. Feizpour, G. S. Thekkadath, S. E. Thomas, J. H. D. Munns, D. J. Saunders, I. A. Walmsley, and J. Nunn, *Quantum Information and Measurement (QIM) 2017* (Optical Society of America, 2017), p. QT2A.4.

[24] J. Iles-Smith, D. P. S. McCutcheon, A. Nazir, and J. Mørk, Nat. Photonics **11**, 521 (2017).

[25] J. H. D. Munns, S. E. Thomas, K. T. Kaczmarek, P. M. Ledingham, D. J. Saunders, J. Nunn, B. Brecht, and I. A. Walmsley, Front. Opt. **2017**, JW4A.16 (2017).

[26] J. Nunn, I. A. Walmsley, M. G. Raymer, K. Surmacz, F. C. Waldermann, Z. Wang, and D. Jaksch, Phys. Rev. A **75**, 011401(R) (2007).

[27] J. Nunn, Quantum memory in atomic ensembles, Ph.D. thesis, University of Oxford, 2008.

[28] O. Lazo-Arjona *et al.* (to be published).

[29] J. Nunn, J. H. D. Munns, S. Thomas, K. T. Kaczmarek, C. Qiu, A. Feizpour, E. Poem, B. Brecht, D. J. Saunders, P. M. Ledingham, D. V. Reddy, M. G. Raymer, and I. A. Walmsley, Phys. Rev. A **96**, 012338 (2017).

[30] R. Grobe, K. Rzazewski, and J. H. Eberly, J. Phys. B **27**, L503 (1994).

[31] M. Gündoğan, P. M. Ledingham, K. Kutluer, M. Mazzera, and H. de Riedmatten, Phys. Rev. Lett. **114**, 230501 (2015).

[32] T. Grange, N. Somaschi, C. Antón, L. De Santis, G. Coppola, V. Giesz, A. Lemaître, I. Sagnes, A. Auffèves, and P. Senellart, Phys. Rev. Lett. **118**, 253602 (2017) .

[33] D. Gammon, E. S. Snow, B. V. Shanabrook, D. S. Katzer, and D. Park, Science **273**, 87 (1996).

[34] K. Sebald, P. Michler, T. Passow, D. Hommel, G. Bacher, and A. Forchel, Appl. Phys. Lett. **81**, 2920 (2002).

[35] C. Couteau, S. Moehl, F. Tinjod, J. M. Gerard, K. Kheng, H. Mariette, J. A. Gaj, R. Romestain, and J. P. Poizat, Appl. Phys. Lett. **85**, 6251 (2004).

[36] M. J. Holmes, K. Choi, S. Kako, M. Arita, and Y. Arakawa, Nano Lett. **14**, 982 (2014).

[37] P. Kaer and J. Mørk, Phys. Rev. B **90**, 035312 (2014).

[38] J. Iles-Smith, D. P. S. McCutcheon, J. Mørk, and A. Nazir, Phys. Rev. B **95**, 201305(R) (2017).

[39] J. Claudon, J. Bleuse, N. S. Malik, M. Bazin, P. Jaffrennou, N. Gregersen, C. Sauvan, P. Lalanne, and J.-M. Gérard, Nat. Photonics **4**, 174 (2010).

[40] M. Arcari, I. Söllner, A. Javadi, S. L. Hansen, S. Mahmoodian, J. Liu, H. Thyrrestrup, E. H. Lee, J. D. Song, S. Stobbe, and P. Lodahl, Phys. Rev. Lett. **113**, 093603 (2014).

[41] J. C. Loredo, N. A. Zakaria, N. Somaschi, C. Anton, L. de Santis, V. Giesz, T. Grange, M. A. Broome, O. Gazzano, G. Coppola, I. Sagnes, A. Lemaitre, A. Auffeves, P. Senellart, M. P. Almeida, and A. G. White, Optica **3**, 433 (2016).

[42] X. Ding, Y. He, Z.-C. Duan, N. Gregersen, M.-C. Chen, S. Unsleber, S. Maier, C. Schneider, M. Kamp, S. Höfling, C.-Y. Lu, and J.-W. Pan, Phys. Rev. Lett. **116**, 020401 (2016).

[43] S. Gerhardt, J. Iles-Smith, D. P. S. McCutcheon, Y.-M. He, S. Unsleber, S. Betzold, N. Gregersen, J. Mørk, S. Höfling, and C. Schneider, Phys. Rev. B **97**, 195432 (2018).

[44] A. V. Kuhlmann, J. Houel, A. Ludwig, L. Greuter, D. Reuter, A. D. Wieck, M. Poggio, and R. J. Warburton, Nat. Phys. **9**, 570 (2013).

[45] L. Besombes, K. Kheng, L. Marsal, and H. Mariette, Phys. Rev. B **63**, 155307 (2001).

[46] I. Favero, G. Cassabois, R. Ferreira, D. Darson, C. Voisin, J. Tignon, C. Delalande, G. Bastard, P. Roussignol, and J. M. Gérard, Phys. Rev. B **68**, 233301 (2003).

[47] E. Peter, J. Hours, P. Senellart, A. Vasanelli, A. Cavanna, J. Bloch, and J. M. Gérard, Phys. Rev. B **69**, 041307 (2004).

[48] Y.-M. He, Y. He, Y.-J. Wei, D. Wu, M. Atatüre, C. Schneider, S. Höfling, M. Kamp, C.-Y. Lu, and J.-W. Pan, Nat. Nanotechnol. **8**, 213 (2013).

[49] Y. J. Wei, Y. M. He, M. C. Chen, Y. N. Hu, Y. He, D. Wu, C. Schneider, M. Kamp, S. Höfling, C. Y. Lu, and J. W. Pan, Nano Lett. **14**, 6515 (2014).